

Lewis Acid–Base Interactions in Weakly Bound Formaldehyde Complexes with CO₂, HCN, and FCN: Considerations on the Cooperative H-Bonding Effects

Roberto Rivelino[†]

Instituto de Física, Universidade Federal da Bahia, 40210-340 Salvador, Bahia, Brazil

Received: October 31, 2007; In Final Form: December 6, 2007

Ab initio quantum chemistry calculations reveal that HCN and mainly FCN can form Lewis acid–base complexes with formaldehyde associated with cooperative H bonds, as first noticed by Wallen et al. (Blatchford, M. A.; Raveendran, P.; Wallen, S. L. *J. Am. Chem. Soc.* **2002**, *124*, 14818–14819) for CO₂-philic materials under supercritical conditions. The present results, obtained with MP2(Full)/aug-cc-pVDZ calculations, show that the degeneracy of the ν_2 mode in free HCN or FCN is removed upon complexation in the same fashion as that of CO₂. The splitting of these bands along with the electron structure analysis provides substantial evidence of the interaction of electron lone pairs of the carbonyl oxygen with the electron-deficient carbon atom of the cyanides. Also, this work investigates the role of H bonds acting as additional stabilizing interactions in the complexes by performing the energetic and geometric characterization.

The acid–base interaction between carbon dioxide and electron-rich chemical systems has long been recognized by Kobatake and Hildebrand¹ since their 1960s studies on gas solubility in different solvents. Over 20 years ago, Sigman et al.² proposed a bond involving π orbitals on CO₂ and the electron lone pairs on the oxygen atom at the carbonyl group by analyzing spectral parameters of solvatochromic indicators in supercritical conditions. Also, the ability of the neutral CO₂ molecule in acting as a mild Lewis acid is well-known in transition-metal complexes.³ Since the past decade, most of these interactions have been studied in polymers with both supercritical and high-pressure CO₂ through infrared spectroscopy.^{4–6} In this direction, Reilly et al.⁷ reported that the interaction of liquid CO₂ with methanol might be ascribed to the Lewis acid–base complexation.⁸

Recently, this interaction has also attracted attention in the low-pressure solubility of substituted carbonyl group polymers⁹ and has been important to rank polymeric materials containing different chain groups.¹⁰ Initial theoretical treatments¹¹ showed that the strength of the complexation energy is in line with the splitting of the ν_2 mode of CO₂ as bound to simple carbonyl compounds. On the basis of several experimental findings, Raveendran and Wallen^{12a} also performed ab initio calculations to understand the chemical nature of the CO₂–carbonyl interaction in synthesized CO₂-philic compounds.^{12b} In this case, in addition to the Lewis acid–base complexation, a C–H \cdots O bond could be formed between the oxygen atoms of CO₂ and the hydrogen atoms of the aldehyde or acetate groups. Actually, this cooperative interaction has been evidenced¹³ by using both Raman spectroscopy and ab initio calculations for the acetaldehyde–CO₂ complex.

Despite its great importance to rationalize the synthesis of renewable materials in “ecological” solvents, CO₂ is not the

unique simple molecule that preferentially can bind to carbonyl groups forming a Lewis acid–base complex. Chemically, one might expect that other small molecules possessing electron-deficient carbon atoms, for example, HCN and FCN, would be potential candidates for also working as Lewis acids in the presence of carbonyl compounds. Although the hazardous and toxic nature of cyanides does not favor a safe use in solute–solvent processes, HCN and FCN play relevant roles in fundamental intermolecular interaction studies.^{14–24} However, none of this research seems to have exploited them acting as Lewis acids, such as it was noticed for the CO₂ interaction with carbonyl groups (Figure 1A). Therefore, the present investigation was carried out using MP2(Full)/aug-cc-pVDZ calculations²⁵ to evaluate the nature and extent of the Lewis acid–base interaction in weakly bound complexes involving formaldehyde and HCN and FCN.

The optimized structural arrangements of the HCHO–CO₂, HCHO–HCN, and HCHO–FCN complexes along with their maps of total electron density are shown in Figure 2 (see also Figure S1 in the Supporting Information). These complexes are supposed to be mostly stabilized by Lewis acid–base interactions, involving the carbonyl oxygen atom in formaldehyde and the electron-deficient carbon atom in CO₂, HCN, or FCN. More realistic than atomic charges, the total electron density in space is not an arbitrary entity, but it is an observable quantity. This elementary fact is noticed along the C=O \cdots C bond (Figure 2) exhibiting the Lewis acid–base complexation. For comparison, some properties of the cyclic formaldehyde dimer,²⁶ involving two C–H \cdots O H bonds, are also calculated (Figure 2D).

In Figure 2A, the total electron density exhibits a relatively large intersection region between the oxygen atom of the carbonyl group and the carbon atom of CO₂. This bonding region gives a fine indication of the electron-donating character of the carbonyl oxygen to the electron-deficient carbon, characterizing a Lewis acid–base interaction in the complex.

[†] To whom correspondence should be addressed. Fax: +55-71-3283 6606. E-mail: rivelino@ufba.br.

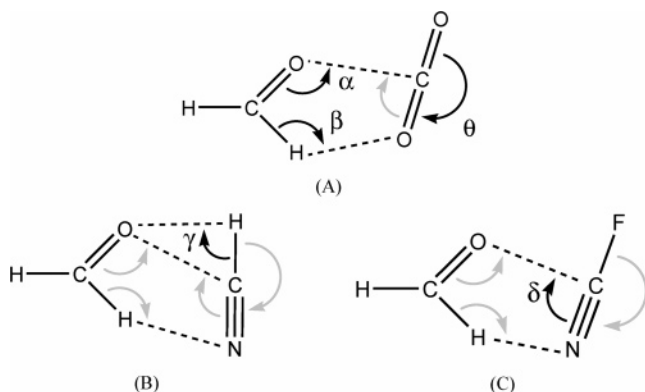


Figure 1. Proposed geometrical structures of the formaldehyde complexes with (A) CO₂, (B) HCN, and (C) FCN involving a typical Lewis acid–base interaction associated with a cooperative C–H···Y (Y = O, N) H bond.

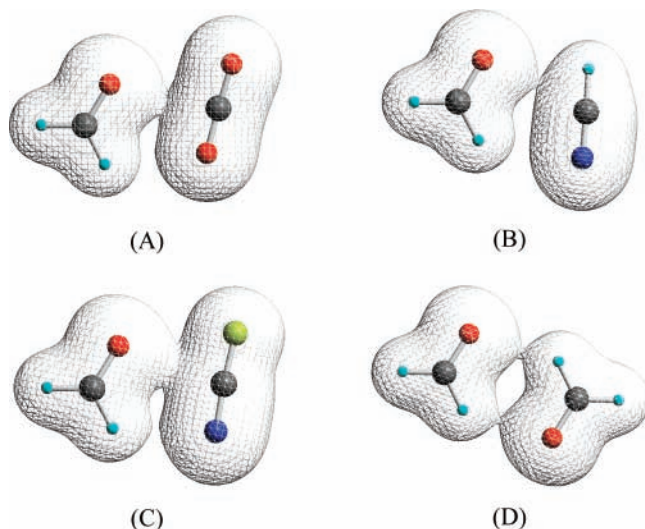


Figure 2. Total electron densities and optimized geometries at the MP2(Full)/aug-cc-pVDZ level of theory. The 0.01 isosurfaces are plotted over a grid of 55 × 55 × 55 points. (A) HCHO–CO₂, (B) HCHO–HCN, (C) HCHO–FCN, and (D) HCHO–HCHO.

For the HCHO–HCN complex (Figure 2B), a smaller intersection region between the two interacting subunits is seen. In this case, there is a bonding region located between the carbonyl oxygen and the middle of the C–H covalent bond of HCN. This can be interpreted as a possible competition between the Lewis acid carbon and the hydrogen atom in binding to the carbonyl oxygen. In Figure 2C, the electron density is more similar to that one obtained for HCHO–CO₂ but exhibits a larger intersection region bridging the carbonyl oxygen to the electron-deficient carbon of FCN.

As suggested by Figure 1, it is also possible to identify H-bond interactions of the type C–H···Y (Y = O, N) shared with the aldehydic proton. Similarly, in the case of HCN, an interaction of the type C–H···O is also expected to be formed with the carbonyl oxygen atom. The necessary geometric parameters to characterize these H bonds are shown in Figure 1. These are the intermolecular bond angles (α , β , γ , δ) and the covalent bond angle (θ), which will be used to assess the nature of all of these interactions (Table 1). Furthermore, these structures define important covalent bond lengths, that is, >C–H and ≡C–H, the H-bond distances, H···Y (Y = O, N), and the intermolecular distances, C···Y (Y = O, N), shown in Table 2.

As discussed above, the calculated values of the geometrical parameters indicate the presence of weak C–H···Y (Y = O,

TABLE 1: Optimized Angles (in degrees) at the MP2(Full)/aug-cc-pVDZ Level (See Figure 1)

angles	HCHO– CO ₂	HCHO– HCN	HCHO– FCN	HCHO– HCHO
θ	178.3	181.7	176.7	
$\Delta\theta$	1.7	–1.7	3.3	
α	109.4	94.3	102.1	
$\beta(\text{C–H}\cdots\text{Y})$	110.8	127.5	118.7	133.5
$\gamma(\text{C–H}\cdots\text{O})$		91.8		
δ	87.1	111.5	100.0	
OCH	121.4	121.5	121.2	121.3

TABLE 2: Optimized Distances (in Å) at the MP2(Full)/aug-cc-pVDZ Level (See Figure 1)

distances	HCHO– CO ₂	HCHO– HCN	HCHO– FCN	HCHO– HCHO
C–H (HCHO)	1.109	1.109	1.109	1.107
$\Delta(\text{C–H})$	–0.001	–0.002	–0.002	–0.003
C=O (HCHO)	1.224	1.226	1.226	1.227
$\Delta(\text{C=O})$	0.002	0.003	0.003	0.004
C=O (CO ₂)	1.181			
C–H (HCN)		1.077		
C≡N		1.182	1.187	
C–F			1.280	
=O···C	2.849	2.944	2.774	
C···Y (Y = O, N)	3.196	3.472	3.237	3.350
H···Y (Y = O, N)	2.630	2.683	2.556	2.490
O···H (HCN)		2.707		

TABLE 3: Different Energy Components (in kcal/mol) Calculated with MP2(Full)/aug-cc-pVDZ

energies	HCHO– CO ₂	HCHO– HCN	HCHO– FCN	HCHO– HCHO
ΔE	–3.31	–4.45	–4.95	–3.95
ΔE^{cp}	–2.39	–3.64	–3.91	–3.12
deformation	0.09	0.05	0.13	0.06
$\Delta Z\text{PVE}$	0.80	0.95	1.06	1.08
ΔE^{cor}	–1.51	–2.64	–2.73	–1.98

N) interactions acting cooperatively to stabilize the complexes. For example, in the three cases, the bond lengths and bond angles are typical of weak H bonds.²⁷ Thus, >C–H (1.109 Å) is much smaller than H···O (2.630 Å) forming a bond angle (β) of $\sim 111^\circ$ in HCHO–CO₂; >C–H (1.109 Å) is much smaller than H···N (2.556 Å) forming a bond angle (β) of $\sim 119^\circ$ in HCHO–FCN; and >C–H (1.109 Å) is much smaller than H···N (2.683 Å) with a bond angle (β) of $\sim 126^\circ$ in HCHO–HCN.

In HCN and FCN complexes, a shortening of 2 mÅ is obtained for the covalent >C–H bond length of formaldehyde. More interesting, the CO₂, HCN, and FCN molecules become slightly bent after being bound. The calculated angles θ of CO₂ and FCN are, respectively, ~ 178 and $\sim 177^\circ$. On the other hand, in the HCHO–HCN complex, this angle is $\sim 182^\circ$, giving rise to a type of six-membered ring complex. Indeed, a secondary ≡C–H···O interaction is expected to be formed in this complex. Hence, this H bond is kept by electrostatic interactions with bond lengths of ≡C–H (1.077 Å) much smaller than those of H···O (2.707 Å) and a bond angle (γ) of $\sim 92^\circ$. Also, this H bond seems to act competitively with the Lewis acid carbon of HCN to stabilize the complex.

Regarding the calculated interaction energies, the BSSE-corrected values (ΔE^{cp}) for the three complexes studied here are –2.39 kcal/mol for HCHO–CO₂, –3.64 kcal/mol for HCHO–HCN, and –3.91 kcal/mol for HCHO–FCN (see Table 3). If one considers only the counterpoise correction, the present value, calculated at the MP2(Full)/aug-cc-pVDZ level, for HCHO–CO₂ is almost the same value of –2.43 kcal/mol as

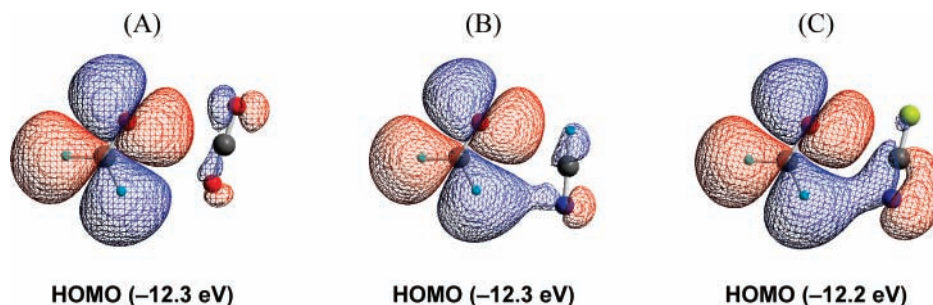


Figure 3. Highest-occupied molecular orbitals (HOMOs) of (A) HCHO–CO₂, (B) HCHO–HCN, and (C) HCHO–FCN complexes. The corresponding orbital energies are given in parentheses.

that obtained by Raveendran and Wallen^{12a} using the MP2/6-31+G*/aug-cc-pVDZ level. Despite this result, a more accurate level was employed here to obtain optimized geometries using appropriate polarized and diffuse basis sets. Taking into account corrections for the geometric deformations and zero-point vibration energies, the expected interaction energies (ΔE^{cor}) are obtained as approximately -1.5 , -2.6 , and -2.7 kcal/mol, respectively (Table 3).

These calculated values indicate that HCHO–HCN and HCHO–FCN have very near binding energies, independent of the imminent H bond ($\equiv\text{C}-\text{H}\cdots\text{O}$) in HCHO–HCN. Notice that these complexation interactions are more than 1 kcal/mol higher compared to those of the HCHO–CO₂ complex. Also, HCHO–HCN and HCHO–FCN are ~ 0.7 kcal/mol more bound than the formaldehyde dimer at the same level of theory. As shown in Figure 2, this dimer contains two $>\text{C}-\text{H}\cdots\text{O}$ H bonds, giving a binding energy of ~ 2 kcal/mol, after all considered corrections (see Table 2). Roughly, this yields an average value of 1 kcal/mol per H bond. Thus, comparing the total interaction of the HCHO dimer to that in HCHO–CO₂, it is possible to estimate a value of ~ 0.5 kcal/mol for the Lewis acid–base contribution. Of course, the value of this specific interaction will be different depending on the nature of the species involved in the complexation. For instance, in HCHO–FCN, the nitrogen atoms can act more effectively as a Lewis base^{15b} moiety than the oxygen atom in HCHO–CO₂.

To better examine the different types of intermolecular bonds in the formaldehyde complexes, some molecular orbitals (derived from correlated calculations) are plotted here in Figures 3 and 4 (see the complete analysis in the Supporting Information). The 0.01 isosurfaces of the highest-occupied molecular orbital (HOMO) for each optimized structure are given in Figure 3. Notice that the HOMO of HCHO–CO₂ is similar to that calculated by Wallen et al.^{12b} for the CO₂–methyl acetate complex, which exhibits both the Lewis acid–base interaction and the cooperative C–H \cdots O bond. Here, for the case of HCHO–HCN, the presence of the cooperative C–H \cdots N bond in the HOMO is much more evident. This is also obvious in the HCHO–FCN HOMO, where the C–H \cdots N bond acts together with the C \equiv N triple bond, introducing further stabilization. The common feature of these interactions is revealed by calculating the HOMO–LUMO electron density differences (Figure S2, Supporting Information).

In Figure 4, the 0.01 isosurfaces of the selected innermost valence molecular orbitals of the complexes are plotted. These HOMO-referenced orbitals are uncommonly delocalized across the whole complexes. In particular, the Lewis acid–base contribution in HCHO–CO₂ can be noticed in the HOMO-5 and the cooperative C–H \cdots O bond in HOMO-8. Conversely, in HCHO–HCN, the HOMO-6 shows the cooperative C–H \cdots N interaction contribution, while the HOMO-7 shows

a competitive character between a possible Lewis acid–base interaction and a secondary C–H \cdots O bond from HCN to HCHO. In HCHO–FCN, the contribution of the interactions seems to be well-separated, as can be seen in HOMO-1 and HOMO-4 exhibiting the Lewis acid–base contribution, in HOMO-6 exhibiting the C–H \cdots N H bond, and in HOMO-8 with both interactions acting cooperatively.

All of the calculated infrared spectra of these complexes at the MP2(Full)/aug-cc-pVDZ level are given in Tables S1–S3 of the Supporting Information. Here, it is important to mention that the calculated harmonic vibrational modes for the isolated CO₂, HCN, and FCN molecules are in good agreement with available experimental data (Table 4). In addition, as can be seen for the doubly degenerate bending vibrations (ν_2), MP2(Full) gives more accurate values than MP2(FC). These results will be useful to evaluate the splitting of ν_2 in the formaldehyde complexes (Table 5). Usually, in the case of the symmetric stretching vibrations (ν_1), no changes have been observed in the infrared spectra, and in the case of the asymmetric stretching vibrations (ν_3), few changes would be expected, as noticed for specific polymer–CO₂ interactions.^{6a}

On the other hand, from the present calculations, it is possible to evaluate any sensitivity of ν_1 and ν_3 to these interactions. Actually, for HCHO–CO₂ and HCHO–HCN, the calculated MP2(Full) shifts in both vibrational modes are, respectively, -1.6 and -1.8 cm⁻¹ in HCHO–CO₂ and -1.9 and -2.1 cm⁻¹ in HCHO–HCN. Indeed, the values of $\Delta\nu_1$ and $\Delta\nu_3$ are within the accuracy to be measured spectroscopically.¹³ In contrast, for HCHO–FCN, these values increase quite significantly to -8.6 and -5.9 cm⁻¹, respectively, at the same level of calculation. Now, these shifts are on the same order of magnitude as those calculated for the C=O stretching mode of formaldehyde after H bonding, which are -4 cm⁻¹ with CO₂, -6 cm⁻¹ with HCN, and -9 cm⁻¹ with FCN.

More noteworthy regarding this issue are the changes in the bending modes (ν_2). As reported in Table 5, the degeneracy of ν_2 is lifted in the complexes. This seems to be directly connected with the interaction between the electron-deficient carbon (the Lewis acid) of CO₂, HCN, or FCN and the carbonyl oxygen of HCHO. However, the splitting is not proportional to the strength of the interaction energy. The largest calculated splitting is obtained for the HCHO–HCN complex (48 cm⁻¹), while HCHO–CO₂ and HCHO–FCN give a very similar splitting of ~ 15 cm⁻¹, although these latter complexes present very different stabilizations (approximately -1.5 and -2.7 kcal/mol, respectively). In addition to the Lewis acid–base interaction, the blue shifts calculated for the symmetric stretch of C–H in HCHO bonded to CO₂, HCN, and FCN are, respectively, 11, 14, and 16 cm⁻¹, indicating the presence of weak, but cooperative, H bonds. In contrast, a blue shift of only 2 cm⁻¹ is obtained for the NC–H symmetric stretch in HCHO–HCN.

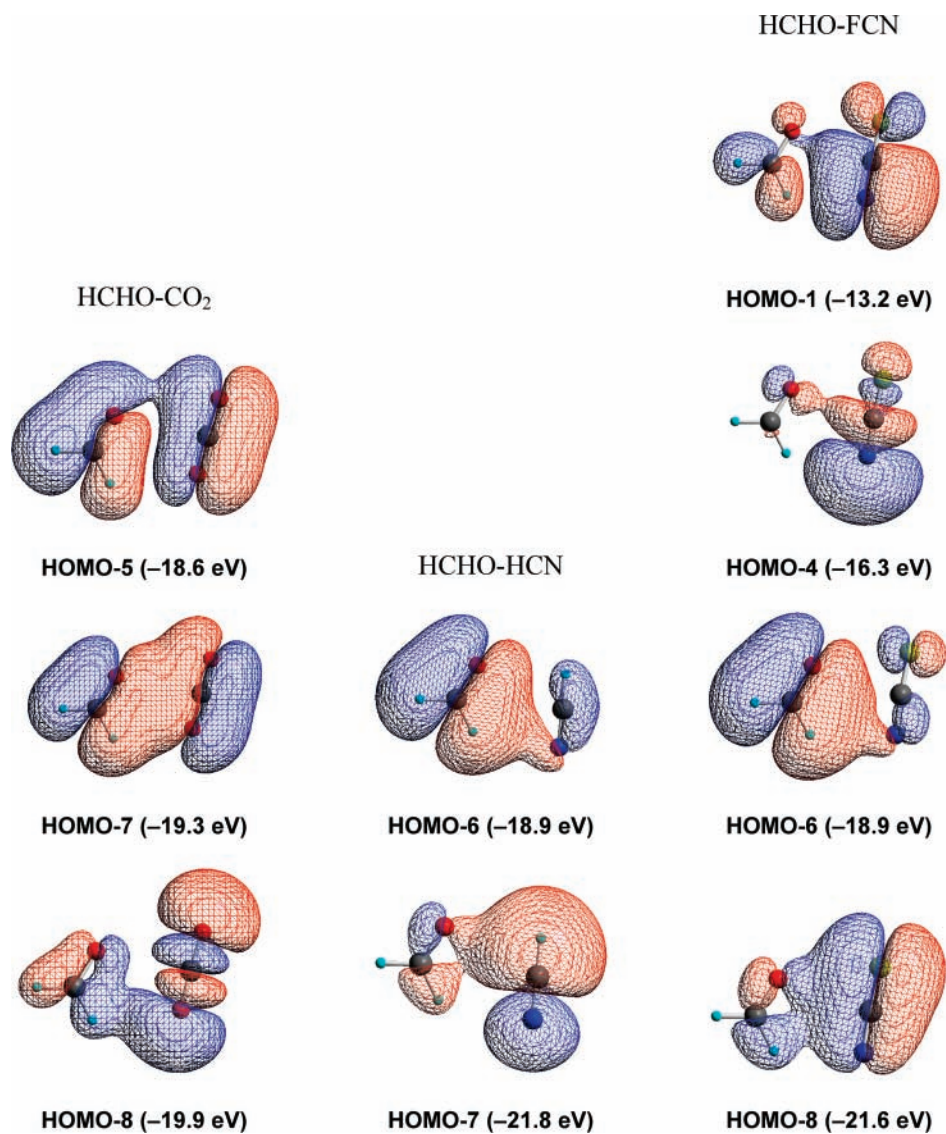


Figure 4. Innermost valence molecular orbitals of the formaldehyde complexes exhibiting different interaction contributions. The corresponding orbital energies are given in parentheses.

TABLE 4: Calculated Harmonic Vibrational Modes (in cm^{-1}) at MP2/aug-cc-pVDZ, with Frozen Core (FC) and All Electrons (Full), in Comparison with Experimental Results

modes	CO ₂			HCN			FCN		
	FC	full	expt. ^a	FC	full	expt. ^b	FC	full	expt. ^c
ν_1	1305.6	1307.2	1388	1990.3	1994.3	2097	1025.3	1026.9	1076
ν_2	655.4	656.4	667	700.4	708.8	712	442.6	444.8	451
ν_3	2379.5	2381.6	2349	3456.7	3463.2	3311	2220.6	2223.9	2319

^a Refs 6a and 4c and <http://vpl.ipac.caltech.edu/spectra/co2.htm>. ^b Ref 19b (and references therein). ^c Ref 23b.

TABLE 5: Calculated Bending Frequencies and Splitting (in cm^{-1}) and the Corresponding IR Intensities (in km/mol) at the MP2(Full)/aug-cc-pVDZ Level

systems	ν_2 splitting (IR intensity)		$\Delta\nu_2$ (Δ IR intensity)
HCHO–CO ₂	641.7 (40)	658.0 (20)	16.3 (–20)
HCHO–HCN	681.1 (44)	729.2 (35)	48.1 (–9)
HCHO–FCN	442.4 (20)	458.2 (6)	15.8 (–14)

In summary, the specific interactions between formaldehyde and CO₂, HCN, and FCN molecules have properly been investigated by employing the MP2(Full)/aug-cc-pVDZ level of theory. The present results show that HCN and FCN form stable complexes like the Lewis acid–base HCHO–CO₂ complex. Usually, HCN is a Brønsted acid or a Lewis base,¹⁶ while FCN is a Lewis base.^{15b} Here, the complex obtained for

HCHO–FCN exhibits the strong amphoteric character of FCN, which can act as both a Lewis base and a Lewis acid. In the case of HCHO–HCN, it appears to have a competition between the Lewis acid–base interaction and two H bonds, C–H \cdots O (from HCN) and C–H \cdots N (from HCHO). Such a complexation involving HCN and aldehydes could be important, for example, to understand the mechanisms of obtaining cyanohydrins.²⁴ Interestingly, from the technological point of view, substituted carbonyl polymer surfaces could be properly used in the sorption process to extract cyanide derivatives from the environment.

Acknowledgment. This work has been partially supported by the Brazilian agencies CNPq and Fapesb (Bahia). The computational calculations were performed in CENAPAD-SP.

Supporting Information Available: Computational details, description of the complete spectra, electron densities, and detailed molecular orbital analysis. This material is available free of charge via the Internet at <http://pubs.acs.org>.

References and Notes

- (1) Kobatake, Y.; Hildebrand, J. H. *J. Phys. Chem.* **1961**, *65*, 331–335.
- (2) Sigman, M. E.; Lindley, S. M.; Leffler, J. E. *J. Am. Chem. Soc.* **1985**, *107*, 1471–1472.
- (3) Halmann, M. M. *Chemical Fixation of Carbon Dioxide, Methods for Recycling CO₂ into Useful Products*; CRC Press: Boca Raton, FL, 1993; p 23.
- (4) (a) Kazarian, S. G.; Hamley, P. A.; Poliakov, M. *J. Am. Chem. Soc.* **1993**, *115*, 9069–9079. (b) Kazarian, S. G.; Gupta, R. G.; Clarke, M. J.; Johnston, K. P.; Poliakov, M. *J. Am. Chem. Soc.* **1993**, *115*, 11099–11109. (c) Yee, G. G.; Fulton, J. L.; Smith, R. D. *J. Phys. Chem.* **1992**, *96*, 6172–6181. (d) Fulton, J. L.; Yee, G. G.; Smith, R. D. *J. Am. Chem. Soc.* **1991**, *113*, 8327–8334.
- (5) (a) Fried, J. R.; Li, W. *J. Appl. Polym. Sci.* **1990**, *41*, 1123–1131. (b) Higuchi, A.; Nakagawa, T. *J. Polym. Sci., Part B: Polym. Phys.* **1994**, *32*, 149–157. (c) Briscoe, B. J.; Kelly, C. T. *Polymer* **1995**, *36*, 3099–3102.
- (6) (a) Kazarian, S. G.; Vincent, M. F.; Bight, F. V.; Liotta, C. L.; Eckert, C. A. *J. Am. Chem. Soc.* **1996**, *118*, 1729–1736. (b) Meredith, J. C.; Johnston, K. P.; Seminario, J. M.; Kazarian, S. G.; Eckert, C. A. *J. Phys. Chem.* **1996**, *100*, 10837–10848.
- (7) Reilly, J. T.; Bokis, C. P.; Donohue, M. D. *Int. J. Thermophys.* **1995**, *16*, 599–610.
- (8) Danten, Y.; Tassaing, T.; Besnard, M. *J. Phys. Chem. A* **2002**, *106*, 11831–11840.
- (9) Sarbu, T.; Styranc, T.; Beckeman, E. *J. Nature* **2000**, *405*, 165–168.
- (10) Nalawade, S. P.; Picchioni, F.; Marsman, J. H.; Janssen, L. P. B. *M. J. Supercrit. Fluids* **2006**, *36*, 236–244.
- (11) Nelson, M. R.; Borkman, R. F. *J. Phys. Chem. A* **1998**, *102*, 7860–7863.
- (12) (a) Raveendran, P.; Wallen, S. L. *J. Am. Chem. Soc.* **2002**, *124*, 12590–12599. (b) Raveendran, P.; Wallen, S. L. *J. Am. Chem. Soc.* **2002**, *124*, 7274–7275.
- (13) Blatchford, M. A.; Raveendran, P.; Wallen, S. L. *J. Am. Chem. Soc.* **2002**, *124*, 14818–14819.
- (14) (a) Larsen, R. W.; Hegelund, F.; Nelander, B. *J. Phys. Chem. A* **2005**, *109*, 4459–4463. (b) Li, R.-J.; Li, Z.-R.; Wu, D.; Hao, X.-Y.; Wang, B.-Q.; Sun, C.-C. *J. Phys. Chem. A* **2003**, *107*, 6306–6310. (c) Rivelino, R.; Canuto, S.; *J. Phys. Chem. A* **2001**, *105*, 11260–11265.
- (15) (a) Burns, W. A.; Leopold, K. R. *J. Am. Chem. Soc.* **1993**, *115*, 11622–11623. (b) Bernardi, F.; Cacace, F.; Occhiucci, G.; Ricci, A.; Rossi, I. *J. Phys. Chem. A* **2000**, *104*, 5545–5550. (c) Jensen, J. O. *J. Mol. Struct.: THEOCHEM* **2005**, *717*, 157–161.
- (16) Pauling, L. *The Nature of the Chemical Bond and the Structure of Molecules and Crystals: An Introduction to Modern Chemistry*; Cornell University Press: Ithaca, NY, 1960.
- (17) (a) Rivelino, R.; Chaudhuri, P.; Canuto, S. *J. Chem. Phys.* **2003**, *118*, 10593–10601. (b) Wang, Z.; Zhang, J.; Wu, J.; Cao, W. *J. Mol. Struct.: THEOCHEM* **2007**, *806*, 239–246. (c) Adrian-Scotto, M.; Vasilescu, D. *J. Mol. Struct.: THEOCHEM* **2007**, *803*, 45–60.
- (18) Muchova, E.; Spirko, V.; Hobza, P.; Nachtigallova, D. *Phys. Chem. Chem. Phys.* **2006**, *8*, 4866–4873.
- (19) (a) Miyakawa, S.; Cleaves, H. J.; Miller, S. L.; *Origins Life Evol. Biosphere* **2002**, *32*, 195–208. (b) Rivelino, R.; Canuto, S. *Chem. Phys. Lett.* **2000**, *322*, 207–212. (c) Rivelino, R.; Ludwig, V.; Rissi, E.; Canuto, S. *J. Mol. Struct.* **2002**, *615*, 257–266.
- (20) (a) Malaspina, T.; Fileti, E. E.; Riveros, J. M.; Canuto, S. *J. Phys. Chem. A* **2006**, *110*, 10303–10308. (b) Sánchez, M.; Provasi, P. F.; Aucar, G. A.; Alkorta, I.; Elguero, J. *J. Phys. Chem. B* **2005**, *109*, 18189–18194.
- (21) Lee, T. J.; Martin, J. M. L.; Dateo, C. E.; Taylor, P. R. *J. Phys. Chem.* **1995**, *99*, 15858–15863.
- (22) (a) Bogey, M.; Farkhsi, A.; Remy, F.; Dubois, I.; Bredohl, H.; Fayt, A. *J. Mol. Spectrosc.* **1995**, *170*, 417–423. (b) Farkhsi, A.; Remy, F.; Dubois, I.; Bredohl, H.; Fayt, A. *J. Mol. Spectrosc.* **1997**, *181*, 119–126. (c) Farkhsi, A.; Remy, F.; Dubois, I.; Bredohl, H.; Fayt, A. *J. Mol. Spectrosc.* **2000**, *201*, 36–55.
- (23) (a) Mishra, S.; Vallet, V.; Poluyanov, L. V.; Domcke, W. *J. Chem. Phys.* **2006**, *124*, 044317. (b) Hu, J. M.; Li, Y.; Zhang, Y. F.; Li, J. Q.; Chen, Y. *J. Mol. Struct.: THEOCHEM* **2005**, *724*, 25–30.
- (24) Gregory, R. J. H. *Chem. Rev.* **1999**, *99*, 3649–3682.
- (25) Frisch, M. J.; Trucks, G. W.; Schlegel, H. B.; Scuseria, G. E.; Robb, M. A.; Cheeseman, J. R.; Zakrzewski, V. G.; Montgomery, J. A., Jr.; Stratmann, R. E.; Burant, J. C.; Dapprich, S.; Millam, J. M.; Daniels, A. D.; Kudin, K. N.; Strain, M. C.; Farkas, O.; Tomasi, J.; Barone, V.; Cossi, M.; Cammi, R.; Mennucci, B.; Pomelli, C.; Adamo, C.; Clifford, S.; Ochterski, J.; Petersson, G. A.; Ayala, P. Y.; Cui, Q.; Morokuma, K.; Malick, D. K.; Rabuck, A. D.; Raghavachari, K.; Foresman, J. B.; Cioslowski, J.; Ortiz, J. V.; Stefanov, B. B.; Liu, G.; Liashenko, A.; Piskorz, P.; Komaromi, I.; Gomperts, R.; Martin, R. L.; Fox, D. J.; Keith, T.; Al-Laham, M. A.; Peng, C. Y.; Nanayakkara, A.; Gonzalez, C.; Challacombe, M.; Gill, P. M. W.; Johnson, B. G.; Chen, W.; Wong, M. W.; Andres, J. L.; Head-Gordon, M.; Replogle, E. S.; Pople, J. A. *Gaussian 98*, revisions A.7 and A.11.4; Gaussian, Inc.: Pittsburgh, PA, 1998.
- (26) (a) Vila, A.; Graña, A. M.; Mosquera, R. A. *Chem. Phys.* **2002**, *281*, 11–22. (b) Gong, X.-L.; Zhou, Z.-Y.; Zhang, H.; Liu, S.-Z. *J. Mol. Struct.: THEOCHEM* **2005**, *718*, 23–29.
- (27) Jeffrey, G. A. *An Introduction to Hydrogen Bonding*; Oxford University Press: New York, 1997.